Particle Sizing in Dense, Rapidly Flowing KCl Suspensions by Photon Migration Techniques

Matthew Bartlett and Huabei Jiang
Dept. of Physics and Astronomy, Clemson University, Clemson, SC 29634

The first experimental measurement of particle-size distribution (PSD) from undiluted, rapidly flowing potassium chloride (KCl) suspensions using continuous-wave photon migration techniques is presented. PSDs were obtained from a laboratory simulation of production-line slurries used in the chemical fertilizer industry. Spectral measurements of concentrated, rapidly flowing slurry containing 25–40% KCl particles were used to calculate the suspensions' reduced scattering coefficient and PSD using inverse algorithms. Our PSD results agree excellently with sieving measurements. Refractive index is important in the calculations of the PSD and the suspensions' reduced scattering coefficient.

Introduction

Many industrial areas, including chemicals, pharmaceuticals, foods, cosmetics, and biotechnology, require a real-time knowledge of their products particle-size distribution (PSD) during production (Allen, 1990). Current particle-sizing methods are often time-intensive or invasive, which remain impractical for monitoring real-time, in-line PSDs. Some optical methods such as dynamic light scattering and extinction-spectrum measurements provide a noninvasive, rapid measurement of PSDs (Kourti et al., 1990; Elicabe and Garcia-Rubio, 1990; Vavra et al., 1995). These methods, however, require dilution of the sample and extensive calibration techniques. Jiang (1998) recently proposed using a continuous-wave (CW) photon migration technique that depends on multiply scattered light to measure the PSD. This technique requires nondilute suspensions, and since absorption and reduced scattering coefficients are calculated separately, no calibration of the measurement is required. This CW-based technique provides an accurate, rapid measurement of the sample's reduced scattering coefficient for further processing to obtain the PSD.

Using this new technique, successful particle-sizing experiments on nondilute, static submicron size TiO_2 suspensions have been demonstrated (Jiang, 1998; Jiang et al., 1998). These experiments have shown that CW photon migration techniques can become a powerful tool for on-line monitoring where the samples are static and particle sizes are small. However, in the chemical fertilizer industry samples usually flow rapidly, consist of large particles, and often change size with time; the PSD must therefore be monitored to ensure the correct final characteristics of the product. Our intent in this study is to demonstrate the extended capability of our technique for measuring the PSD of large particles under rapid-flow conditions. Toward this end, together with Potash Corporation (Saskatoon, Canada), we developed a laboratory simulation of on-line fertilizer production. The sample consisted of a fertilizer slurry made up of saturated potassium chloride (KCl) solution and 25–45% KCl particles. After these elements were combined in a cylindrical container, a magnetic stirring device was used to rapidly stir the suspension. From the spectral measurements of the reduced scattering coefficient, μ_s', a successful PSD was obtained using an inverse computer algorithm. Our PSD calculations have been compared with the PSD obtained from sieving measurements, and these results have demonstrated excellent agreement between the two. We have also discussed the impact of the sample's refractive index on the PSD reconstruction.

Experiment

Our CW photon migration system is shown in Figure 1. In this system, the light source consists of a 100-W tungsten halogen lamp and a fiber-optic cable. Sixteen detection fibers collect the diffuse reflectance and send the collected light signals to the detection system for automatic data recording,

Correspondence concerning this article should be addressed to H. Jiang.

which consists of a spectrograph (Triax 320, ISA, Edison, NJ), a liquid-nitrogen-cooled, 2000×800-pixel CCD camera (Spectrum One, ISA, Edison, NJ), and a PC. A lens focuses the light onto the tip of the fiber that delivers the light to the sample. Theory requires the source and detection fibers to be in the same plain along the surface of the slurries. This has been accomplished by developing a solid cylindrical fiber-optic probe containing both source and detection fibers (see Figure 2). The 200-μm-diam fibers extend through a thin metal plate on the end of the probe. The first 9 detection fibers are evenly spaced in 1-mm increments radially from the source fiber, and the farthest 7 detection fibers are spaced from 23 mm to 28 mm from the source.

The sample consisted of deionized water, KCl powder, and the KCl fertilizer particles, which ranged in size from 10 μm to 2,000 μm. The KCl powder dissolves in the water until saturation occurs, providing a stable medium for the KCl particles. Twenty-five to 45% (by wt.) of KCl fertilizer particles were then added to the saturated solution. Two hundred mL of the combined ingredients were placed in a 250-mL Pyrex flash. In order to simulate a rapidly flowing homogeneous mixture, a magnetic stirring device mixed the sample at high revolutions. Mixing presented two substantial problems: first, swirling mixture produced a vortex similar to that seen when a sink or tub are rapidly drained; second, the heavier fertilizer particles moved to the inside of the glass, leaving mostly pure solution with few particles under the light probe. To remove the vortex and enhance a homogeneous mixture, two metal baffles were attached to the inside of the glass, as illustrated in Figure 3. Lowering the probe slightly into the solution also prevented the vortex. The combination of magnetic mixers and baffles produced the mixture needed to obtain an accurate measurement of the reduced scattering coefficient, μ_s', and absorption coefficient, μ_a. Although contrived for the lab, this optically based method appears to meet the industry criteria for rapidly flowing, nondilute particle sizing.

After the data have been collected, the detection system converts each fiber's light into a data file consisting of light intensity vs. wavelength (see Figure 4). The intensity from the first fiber is used to normalize all the fibers. Graphing this normalized intensity vs. the radial distance produces an exponentially decreasing curve for each wavelength (see Figure 5). The optical properties algorithm performs a nonlinear, least-square fit of the intensity vs. distance curve to obtain μ_s' and μ_a. The particle-sizing algorithm uses this calculated μ_s' to derive the sample's PSD.

Theory

Obtaining the PSD of a sample requires the following two-step process: (1) determine the reduced scattering coefficient at multiple wavelengths using diffusion theory (Groenhuis et al., 1983), and (2) use the reduced scattering coefficient spectrum to calculate the PSD. Farrell and Patterson (1992) used the diffusion equation describing photon transport in turbid media to obtain the radially dependent diffuse reflectance of light for a semi-infinite medium where the extrapolated or type III boundary conditions were used: $\Psi(r) - 2AD\hat{\Omega}_n \cdot \nabla\Psi(r) = 0$, where $\Psi(r)$ is the fluence rate or photon density, D is the diffusion coefficient, $\hat{\Omega}_n$ is the unit normal directed into the sample, and A is related to the internal reflection. When the reflectance is normalized and measured along the surface, the solution to this diffusion

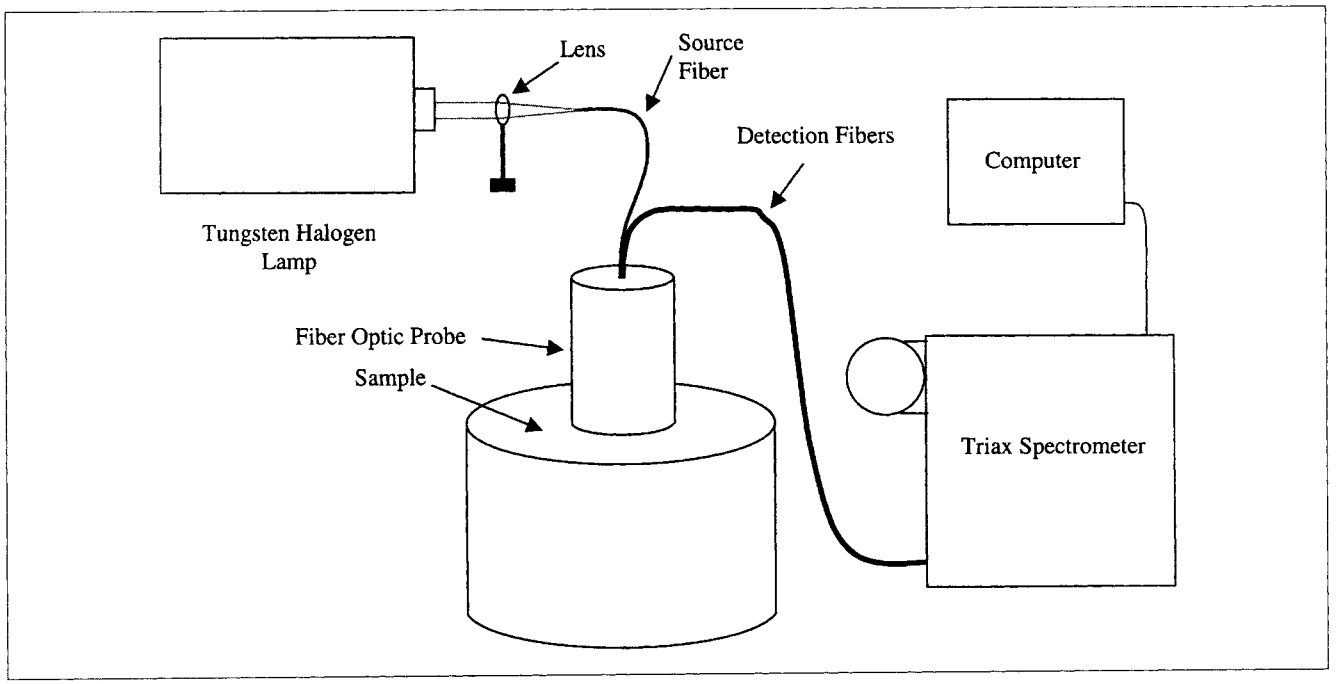

Figure 1. Experimental setup used to obtain the PSD.

Light from a tungsten halogen lamp is focused by a lens onto a fiber-optic cable. This source fiber delivers light to the sample. The probe transmits collected light to the CCD interfaced to a computer.

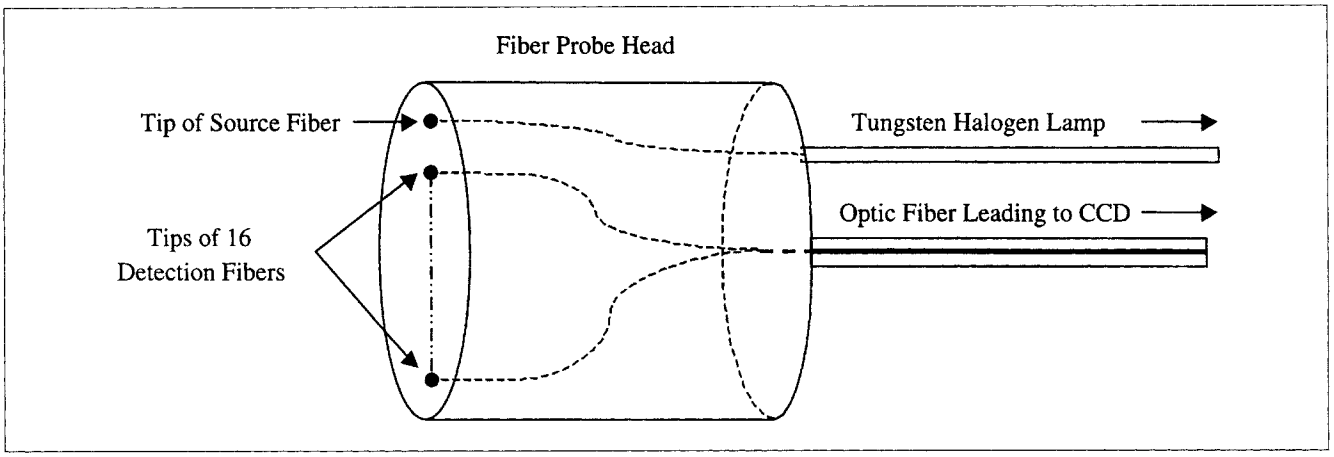

Figure 2. Solid cylindrical probe with both source and detection fibers.

The black dots represent the tips of the source and detection fibers. The source fiber delivers light from the tungsten halogen lamp. Only 2 of the 16 detection fibers are shown. The internal dotted lines indicate the fiber-optic cables that transfer the collected light to the CCD.

equation relies entirely upon the reduced scattering coefficient, μ_s', and absorption coefficient, μ_a. The normalized reflectance, $(R(\rho))^c$, can be calculated at multiple detection positions along the sample's surface. Performing a least-square minimization between the measured reflectance, $(R(\rho))^m$, and the calculated reflectance, $[R(\rho)]^c$, leads to $\chi^2 = \sum_{i=1}^{m}[(R(\rho))_i^m - (R(\rho))_i^c]^2$, where M represents the number of detection fibers. Using Newton's method the optical properties can be iterativley updated using systems of equations represented by $\tilde{J}^T\tilde{J}(\Delta\zeta) = \tilde{J}^T\{[R(\rho)]^m - [R(\rho)]^c\}$, where the Jacobian matrix $(\tilde{J})$ represents the sensitivity of reflectance measured at multiple distances (x_i) and $\Delta\zeta$ up-

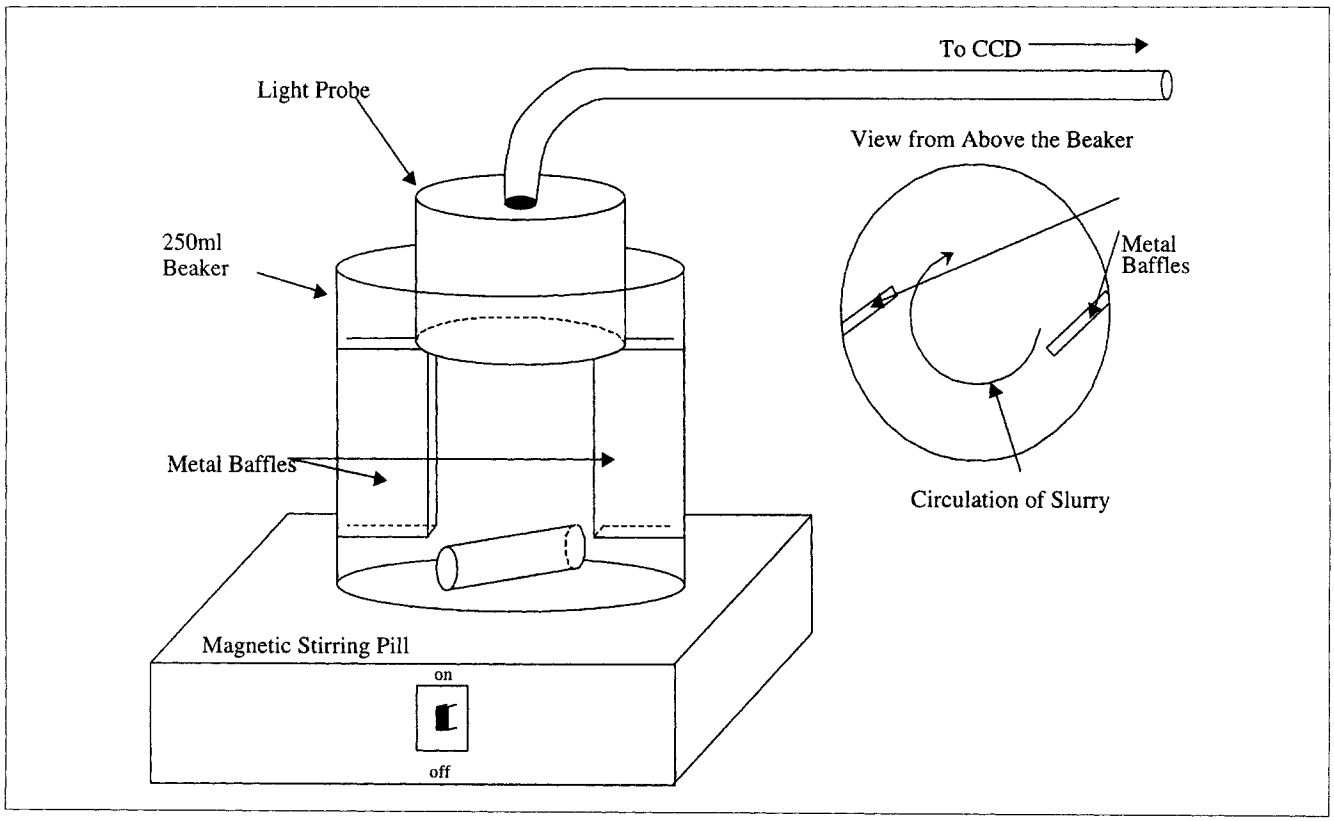

Figure 3. Left picture representing Pyrex beaker with the fiber with the fiber probe on top.

Two metal baffles are attached to the inside of the glass. In the bottom of the beaker is a cylindrical, magnetic stirring pill controlled by the box underneath. The right picture provides a top-down view of the Pyrex jar with baffles.

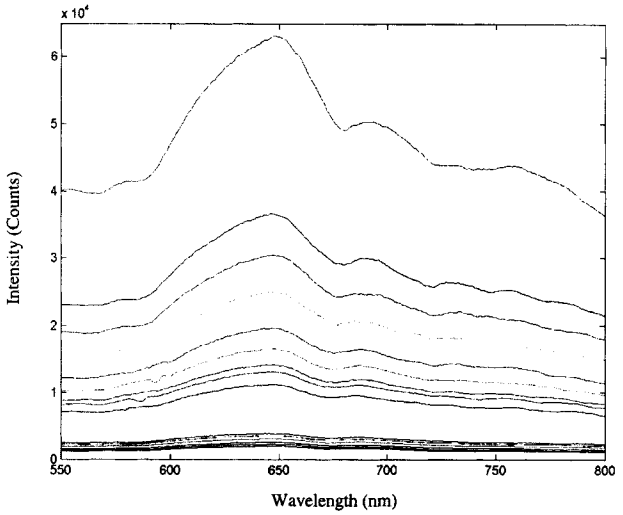

Figure 4. Sixteen curves of light intensity vs. wavelength from the 25% sample of KCl.

There is one curve for each fiber. From highest intensity to lowest, the curves represent the fibers nearest the source to the farthest away.

dates μ_s' and μ_a. Inverting the matrix $\tilde{J}^T\tilde{J}$ directly to obtain $\Delta\zeta$ is usually impossible, since the matrix is ill-conditioned. We used a Marquardt-type regularization scheme to overcome this problem, which adds a scalar parameter, α, to the diagonal elements of the $\tilde{J}^T\tilde{J}$ matrix. The stability of μ_s' relies heavily on the value of α and the amount it is reduced each iteration. Using this method the optical properties for 2000 separate wavelengths of from 550 nm to 800 nm can be calculated. Figure 6 shows the reduced scattering coefficient spectrum measured for the 25% KCl sample.

Once an accurate value of μ_s' has been calculated, the particle-size distribution can be derived using the following equation:

$$\mu_s'(\lambda) = \int_0^\infty \frac{3Q_{\text{scat}}(x,n,\lambda)(1-g(x,n,\lambda))\phi f(x)\,dx}{2x}, \quad (1)$$

where $\mu_s'(\lambda)$ is the wavelength-dependent reduced scattering coefficient, g is the mean cosine of the scattering angle, Q_{scat} is the scattering efficiency, n is the refractive index of the medium, λ is the wavelength of light, $f(x)$ is the particle-volume size distribution, x is the diameter of the particles, and ϕ is the total volume fraction of particles. Here, Q_{scat} and g can be calculated from Mie theory. For many practical process streams, the PSD usually can be well approximated with a Gaussian or lognormal, *a priori* distribution. The shape of these distributions is controlled by three parameters a, b, and c, which determine the amplitude, width, and mean position of the curve, respectively. Since these three parameters are not independent, this provides an actual two-parameter equation for calculating μ_s'. Again using a least-square fit between the observed $(\mu_s')^m$ and the calculated $(\mu_s')^c$ leads to $X^2 = \Sigma_{i=1}^N[(\mu_s')_i^m - (\mu_s')_i^c]^2$, where N is the number of wavelengths. Using Newton's method and a Marquardt-type regularization leads to $[\tilde{J}^T\tilde{J}(\Delta\xi) + \alpha I] = \tilde{J}^T[(\mu_s')^m - (\mu_s')^c]$. Here $\tilde{J}$ represents the sensitivity of the reduced scattering coefficient with respect to ξ; I is the identity matrix; α regularizes the ill-conditioned matrix product $\tilde{J}^T\tilde{J}$; and $\Delta\xi$ is the perturbation vector that updates the particle-sizing parameters a, b, and c. When the measured $(\mu_s')^m$ is accurate, the particle-size distribution can be calculated within approximately 30 iterations. Both algorithms just described use a least-square minimization procedure to adjust the parameters until the observed and calculated data match as closely as possible. Using these algorithms, both the reduced scattering coefficient and the particle-size distribution have been obtained accurately, as demonstrated in the following results section.

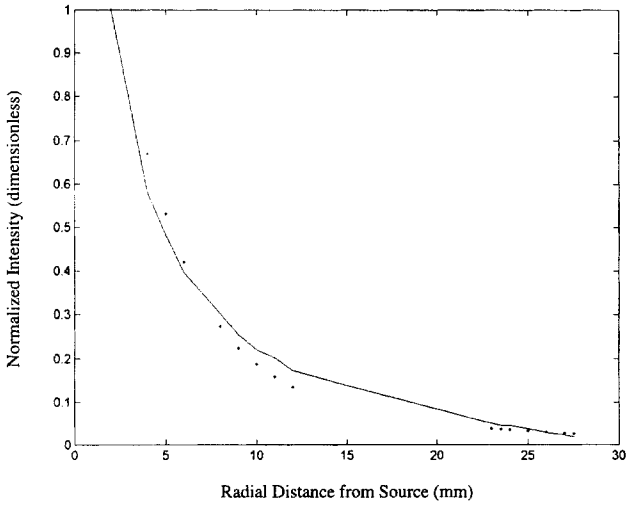

Figure 5. 25% sample with normalized intensity for 16 collection fibers at one wavelength (600 nm).

Each intensity is graphed vs. the detector's radial distance from the source fiber.

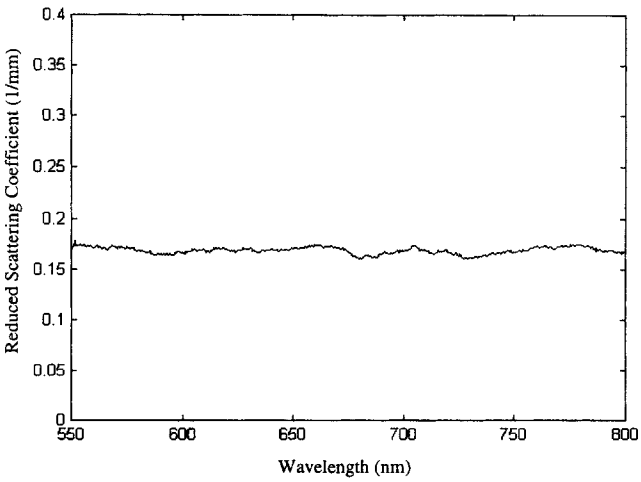

Figure 6. μ_s' vs. wavelength obtained from the 25% sample.

This μ_s' was used by the particle-sizing algorithm to obtain the size distribution.

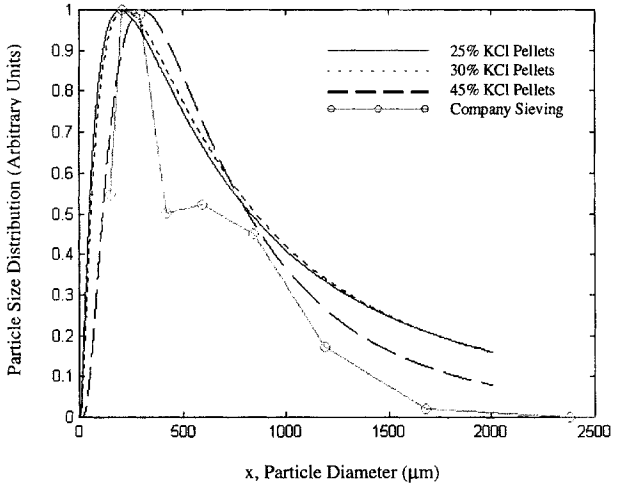

Figure 7. Particle-size distribution, $f(x)$ (arbitrary units), as a function of diameter, x, (μm) produced by 25%, 30%, and 45% KCl samples.

Obtained from the reduced scattering coefficient by the PSD algorithm using *a priori* log normal distribution.

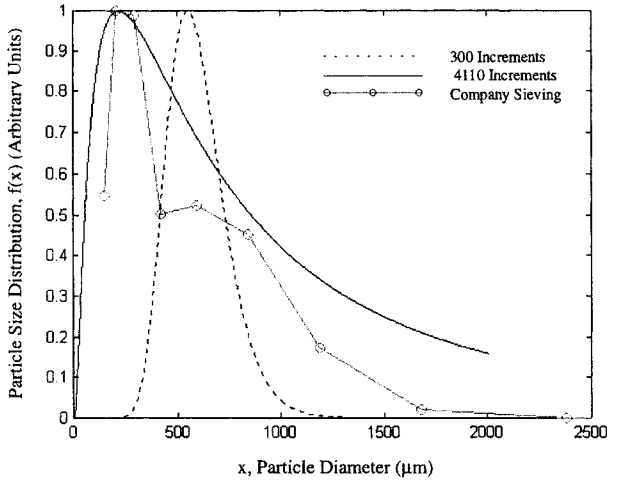

Figure 8. Particle-size distribution, $f(x)$ (arbitrary units), as a function of diameter, x, (μm) produced by a 25% KCl sample.

The solid line with circles came from a sieving measurement. The same file produced both dotted and solid curves, but the dotted line was produced using 300 increments to discretize Eq. 1 and the solid line used 4110.

Results

CW photon migration measurements performed on rapidly flowing KCl samples produced PSDs that matched excellently with the PSD obtained from sieving. The sample was tested at three different concentrations of 25%, 30% and 45%. As can be seen from Figure 7, the PSD did not vary significantly with concentration. Variation of PSD between percentages may be due in part to fluctuations in the homogeneity of the solution while stirring. Lower percentages of particles may not mix as well as more concentrated slurries. Also, since the PSD algorithm currently relies heavily on a discretization of the integral in Eq. 1 in the theory section, finer incrementation may be needed to obtain accurate distributions at large particle sizes. In this study, the integral for the sample was discretized as follows: 3,000 increments between 1 and 901 μm, and 1110 increments between 901 and 2,011 μm. The scattering efficiencies calculated by this level of discretization produced files in excess of 100 megs, increasing the time required for particle sizing. Coarser increments produced significantly worse results, as demonstrated in Figure 8. We are currently studying more efficient methods for performing this integral computation.

In order to use diffusion theory to calculate μ_s' as described in the theory section, a constant known as the relative reflective index ($RNR = n_{\text{sample}}/n_{\text{probe}}$) must be given (Farrell and Patterson, 1992). This research indicates that μ_s' depends considerably on the correct value of RNR, as shown in Figure 9, and therefore the PSD is also effected as displayed in Figure 10. As RNR changes, the μ_s' spectrum shifts to higher or lower values, but it maintains the same general shape as evidenced in Figure 9. Since the slurry consisted of a solution with refractive index $n = 1.34$ and KCl particles with $n = 1.49$, the average refractive index for the slurry was calculated to be $n_{\text{sample}} = 1.41$. The reflective index of our probe is $n_{\text{probe}} = 1.15$, resulting in an RNR value of approximately 1.23. As demonstrated in Figure 10, the best fit of the sieving was produced by the $RNR = 1.20$.

Discussion and Conclusions

The results of this study clearly indicate the applicability of CW photon migration techniques for determining the PSD of rapidly flowing, nondilute, large-particle samples. Although primarily focused on the fertilizer industry, this study demonstrates a powerful particle-sizing procedure with the following essential characteristics: easy implementation resulting from no need to calibrate for wavelength-dependent absorption, minimal time to collect data, the multiply scattering light measurement negating sample dilution, and a noninvasive probe suitable for on-line product monitoring. This prelimi-

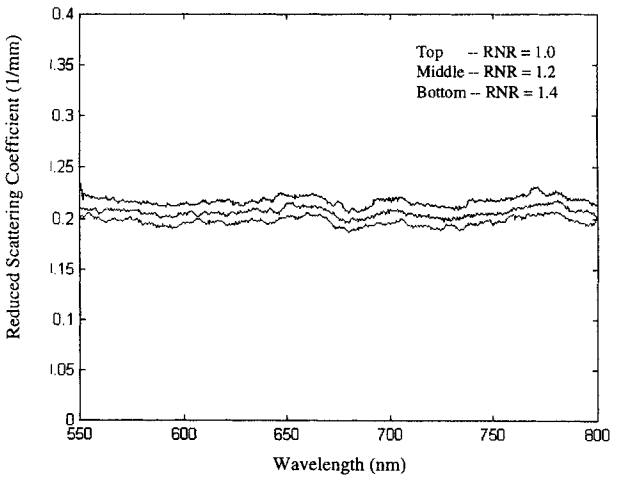

Figure 9. Experimental results of μ_s' vs. wavelength obtained from 30% KCl particles for three separate values of RNR.

For the top curve RNR = 1.0; for the middle curve RNR = 1.2; for the bottom curve RNR = 1.4. Changing RNR shifts μ', but the curve has the same general trend.

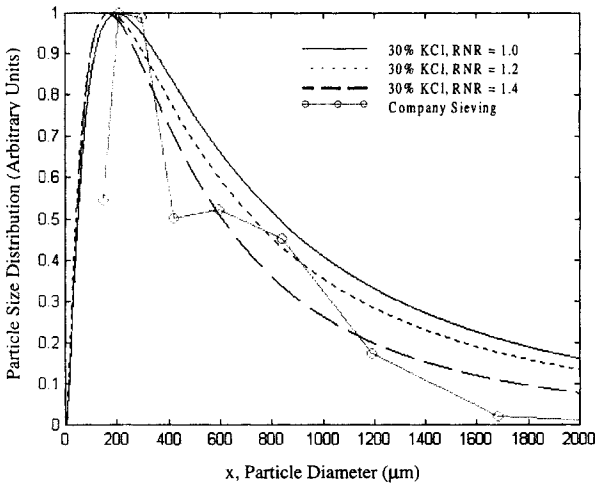

Figure 10. Particle-size distribution, $f(x)$ (arbitrary units), as a function of diameter, x, (μm) produced by a 30% KCl sample.

The PSD varied with RNR. The dotted line has RNR = 1.0; the solid line has an RNR = 1.2; the dashed line has a RNR = 1.4. The solid line with circles is from the sieving.

nary study has also revealed two areas that could improve the technique. First, since in some cases the actual refractive index, n, may be difficult or impossible to be known as *a priori*, an alternative way will be needed to calculate it. In this regard, we could treat *RNR* as a third parameter that can be reconstructed in the algorithm for determining optical properties. Of course, this warrants further studies. Second, a large range of particle diameters, such as 10 μm–2000 μm, produces extremely large files when the integral in Eq. 1 is discretized, increasing the time needed to calculate the PSD. Alternative methods for performing this integral exist (Press et al., 1994), but warrant further study. Nonetheless, we have demonstrated in this study that this CW photon migration technique holds great promise for on-line, noninvasive monitoring of particle-size distributions for rapidly flowing particles.

Acknowledgments

We thank Dr. Wey Lee of Potash Corporation (Saskatoon, Canada) for providing us KCl samples and the sieving measurements.

Literature Cited

Allen, T., *Particle Size Measurement*, 4th ed., Chapman & Hall, New York, 1990.

Elicabe, G. E., and L. H. Garcia-Rubio, "Latex Particle Size Distribution from Turbidimetric Measurements," *Polymer Characterization*, ACS Advances in Chemistry Series, Vol. 227, C. Carver and T. Provder, eds., American Chemical Society, Washington, DC, p. 83 (1990).

Farrell, T. J., and M. S. Patterson, "A Diffusion Theory Model of Spatially Resolved, Steady-State Diffuse Reflectance for the Noninvasive Determination of Tissue Optical Properties In Vivo," *Med. Phys.*, **19**, 879 (1992).

Groenhuis, R. A. J., H. A. Ferwerda, and J. T. Bosch, "Scattering and Absorption of Turbid Materials Determined from Reflection Measurements: 1. Theory," *Appl. Opt.*, **22**, 2456 (1983).

Jiang, H., G. Marquez, and L. Wang, "Particle Sizing in Concentrated Suspensions by Use of Steady-State, Continuous-Wave Photon-Migration Techniques," *Opt. Lett.*, **23**, 394 (1998).

Jiang, H., "Enhance Photon-Migration Methods for Particle Sizing in Concentrated Suspensions," *AIChE J.*, **44**, 1740 (1998).

Kourti, T., J. F. MacGregor, A. E. Hamielec, D. F. Nicoli, and V. B. Elings, "On-Line Particle Size Determination During Latex Production Using Dynamic Light Scattering," *Polymer Characterization*, ACS Advances in Chemistry Series, Vol. 227, C. Carber and T. Provder, eds., American Chemical Society, Washington, DC (1990).

Press, W. H., S. A. Teukolsky, W. T. Vetterling, and B. P. Flannery, *Numerical Recipes in Fortran*, Cambridge Univ. Press, New York, 1994.

Vavra, J. J. Antalik, and M. Liska, "Application of Regression Analysis in Spectroturbidity Size Characterization Methods," *Part. Part. Syst. Charact.*, **12**, 38 (1995).

Manuscript received Sept. 8, 1999, and revision received June 26, 2000.